Effect of CFRP Bonded Length on the Strength of Axially loaded HSS

Mostafa Atteya[1], Amr Shaat[2] and Ezzeldin Sayed-Ahmed[3]

1. *Postgraduate student, Ain Shams University, Egypt*
2. *Professor (Associate) of steel structures The German University in Cairo (On leave from Ain Shams University), Egypt*
3. *Professor of steel structures -The American University in Cairo (On leave from Ain Shams University), Egypt*

الملخص

يمكن زيادة قدرة التحميل المحوري وصلابة الأعمدة الحديدية المفرغة مربعة الشكل عن طريق لصق ألواح الياف الكربون المدعمة بالبوليمرات على سطح الأعمدة . أظهرت الأبحاث المعملية حالتي انهيار مختلفة وهما الانفصال ما بين العنصر المدعم والواح الدعم, وانهيار ألواح الياف الكربون المدعمة بالبوليمرات نفسها . وتعتمد فاعلية طريقة التدعيم هذه على عدة عناصر منها (نحافة العنصرالانشائي الصلب, قطاع ألواح الياف الكربون المدعمة بالبوليمرات, طول ألواح الياف الكربون المدعمة بالبوليمرات, خصائص ألواح الياف الكربون المدعمة بالبوليمرات, خصائص المادة اللاصقة). ويتناول هذا البحث دراسة طريقة التدعيم المذكورة أعلاه عن طريق استخدام نموذج رياضي وطريقة التحليل العددي لمحاكاة السلوك الفعلي للنماذج المعملية المقدمة في بحث (شعث وفام 2009) , ويدرس هذا النموذج العددي تأثير كل من, طريقة تصنيع العنصر الانشائي الصلب, اللاخطية الكامنة في تمثيل المواد الإنشائية , الخلل الذي قد ينشأ في أبعاد العنصر الإنشائي. وقد تم عمل دراسة بارامترية عن طريق اشتخدام طريقة العناصر المحددة للتنبأ بفاعلية تغيير طول ألواح الكربون المدعمة بالبوليمرات.

ABSTRACT

The axial load capacity and the stiffness of a rectangular hollow structural section (HSS) can be increased by adhesively bonding carbon fiber reinforced polymer (CFRP) plates to the outer surface of the steel tube. Experimental studies showed that two different failure modes generally occur for such a strengthened tube, the first mode was debonding of CFRP layer on the compression side of the buckled column. The second mode is crushing of CFRP layer on the compression side of the column. The effectiveness of this strengthening method depends on many parameters (steel tube slenderness, CFRP cross sectional area, CFRP length, CFRP properties, and properties of the adhesive). This paper presents a finite element FE study of such strengthening technique, first by validating the FE model against the experimental work by Shaat and Fam (2009), in which the consequences of the manufacturing process, strain-hardening of the material, geometric imperfections, residual stresses in the section, and interaction between steel and CFRP plates are explicitly accounted for. Followed by a parametric study using the FE model to estimate the effectiveness of CFRP length.

KEYWORDS: HSS, local Imperfections, global imperfections, residual stresses, cold-formed, traction-separation model, CFRP

INTRODUCTION

Shaat (2007) conducted an experimental research program to investigate the performance of steel structures retrofitted using CFRP sheets under axial compression load. The purpose was to study the effect of the slenderness ratio of the column on the axial compressive behavior of slender HSS steel columns strengthened using different types of CFRP sheets and plates. The specimens were divided into six sets, three identical specimens each; total of 18 steel columns, the columns were fabricated using HSS1 section (44 x 44 x 3.2 mm); sets A1, A3, and A5 served as control (unstrengthened) sets with slenderness ratios of 46, 70, and 93, respectively; while sets A2, A4, and A6 were the corresponding strengthened sets where CFRP strips were bonded longitudinally on each of the two opposite sides of all specimens in these sets. An analytical model introduced by Shaat and Fam (2009) that was used to predict the axial load capacity of the slender steel columns strengthened using longitudinal CFRP layers.

This paper introduces a numerical model to investigate behavior and strength of CFRP strengthened slender HSS steel columns. Investigated strengthened columns had slenderness ratios ranging between 46 and 70. In this slenderness range, strengthened columns failed due to debonding of the CFRP layers on the compression side of the buckled column.

The Numerical Model

The numerical model was implemented using the finite element package Abaqus, and was applied to study the structural behavior of the axially loaded carbon steel cold-formed HSS strengthened using bonded CFRP reinforcement oriented in the longitudinal direction see Figure 15 (a and b).

The material model, initial geometric imperfections, residual stresses and associated equivalent plastic strains, as well as interaction between cold-formed HSS and CFRP plate were all considered. Columns were modeled with 3mm S4R shell elements, the column corners consisted of 3 elements. Simpson's rule was used for the integration through the shell thickness, and 21 section (integration) points were specified across the thickness of the shell element see Figure 15 (c).

The hinged ends of the column were modeled as a rigid end plate with the translational degrees of freedom U1, U2, and U3 restrained along the middle line of the rigid plate for the bottom plate, while degrees of freedom U1 and U2 where restrained for the top hinge.
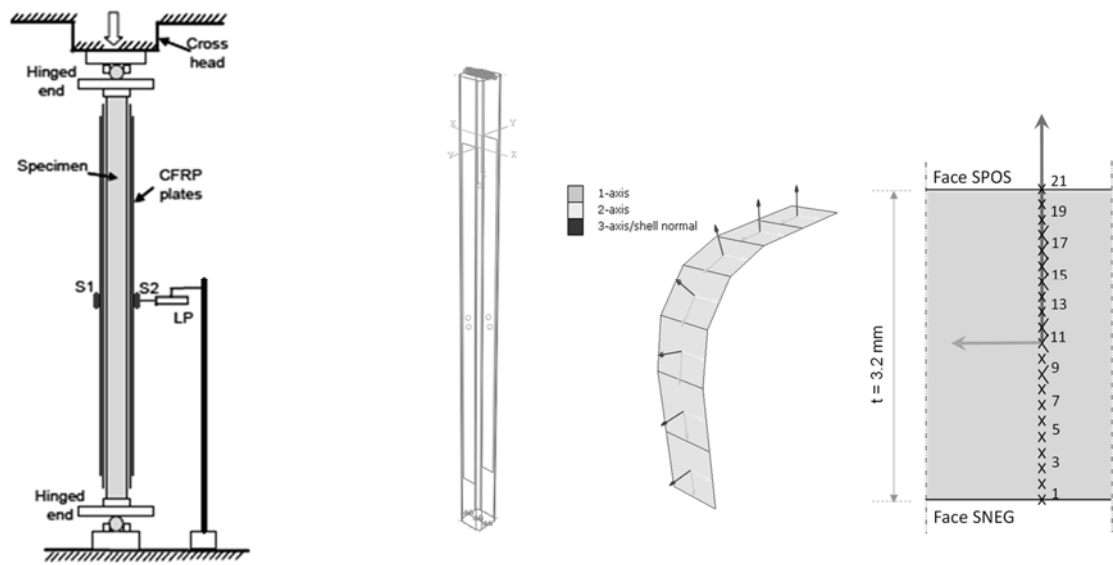
(a) Experimental test setup　(b) Numerical Model setup　(c) Corner mesh and section points

Figure 15: Experimental test setup and numerical model

Initial Geometric Imperfections

Shape: for members under compression it is preferred to consider both local and global imperfections in the modeling of the geometric imperfections. To take account for the interaction between local and global buckling modes, imperfections were introduced into the FE model by scaling the lowest eigenmodes.

Amplitude: for providing reasonably conservative fit to the test data for cold-formed carbon steel sections, the global imperfection amplitude of the structural member is set as 1/1500 times the member length, while the local imperfection amplitude of the cold-formed member has been defined as 0.1 times the plate thickness.

Residual Stresses

Prediction of residual stresses in cold-formed sections can, thus, be separated into two steps: the residual stresses from the coiling and uncoiling process involving pure bending of the steel sheet and residual stresses from the cold-bending process.

The residual stresses and equivalent plastic strains from both processes are determined analytically Cristopher and Schafer (2009), and applied as predefined fields in the numerical model (initial stresses and equivalent plastic strains defined through section thickness).

In this method, a single stress-strain curve of the unbiased virgin material is used for both flat and corner regions of a cold-bending section.
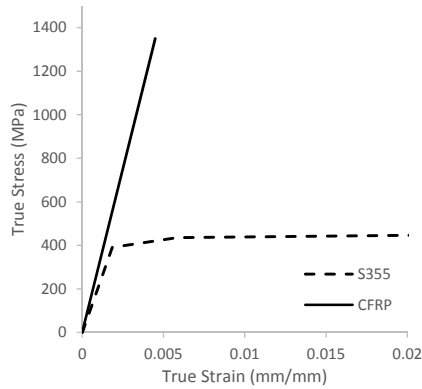
Figure 16: Tensile stress-strain curve for steel and CFRP

HSS - CFRP Interaction properties

HSS-CFRP adhesive layer was modelled using surface-based cohesive behaviour provided by Abaqus. The cohesive behaviour was represented by a traction-separation equation ($\sigma - \delta$) replacing the classical engineering stress-strain ($\sigma - \varepsilon$) equation Barbero (2013).

The traction-separation model in Abaqus assumes an initial linear elastic behavior followed by the initiation and evolution of damage as shown in Figure 17:

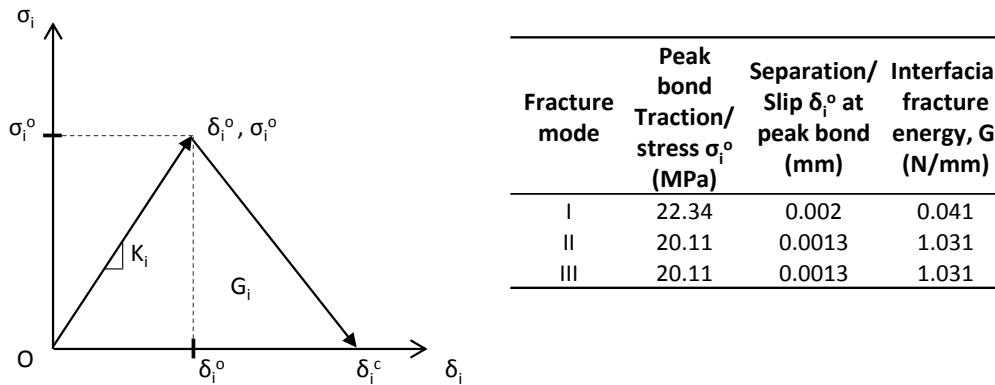| Fracture mode	Peak bond Traction/ stress σ_i^o (MPa)	Separation/ Slip δ_i^o at peak bond (mm)	Interfacial fracture energy, G_i (N/mm)
I	22.34	0.002	0.041
II	20.11	0.0013	1.031
III	20.11	0.0013	1.031

Figure 17: Traction-Separation model and values for cohesive zone model (Fernando et al. 2012)

Since Plate end debonding is governed by both interfacial normal stresses (mode I) and interfacial shear stresses (mode II), Benzeggagh-Kenane (BK) mixed mode behavior was defined with 1.75 power to consider the effect of interaction between mode I loading and mode II loading Barbero (2013). Viscous regularization of the constitutive equations of 0.001 was considered to overcome some of the severe convergence difficulties.

Analysis Methodology

Analysis methodology consisted of three steps. The first stage is a linear eigenvalue buckling analysis performed on the "perfect" column to establish probable buckling modes. Lanczos eigensolver was used to extract the linear buckling modes. Lowest global and local buckling modes were then scaled and superposed to define initial geometrical imperfections. The objective of this stage is to trigger the buckling of the column under concentric compressive load and to determine the most critical imperfection shape that leads to the lowest collapse load of rectangular HSS. The second stage introduces the geometric imperfections obtained in the first stage as well as the residual stresses and equivalent plastic strains explicitly into the numerical model. The final stage is a nonlinear static analysis on the "imperfect" column carried out using the modified Riks method to obtain the ultimate load and the failure mode of the column. The Riks algorithm was adopted to overcome the above mentioned severe convergence problems and to be able to predict the postbuckling behavior via the snap-back/snap-through capabilities

Verification of the Numerical Model

The FE results were compared with the experimental research data published by Shaat and Fam (2009) to verify the model before using it in the parametric study. Table 6 summarizes the load capacities obtained from the FE models of control specimens (A1, A3, and A5) and the strengthened specimens (P1, P2, and P3). The finite element ultimate loads P_{FEA} matched well with the experimental ultimate load P_{Exp} showing a variation of about 6%.

Specimen	HSS length (mm)	Slenderness ratio	Specimen type	CFRP		Ultimate load (kN)		Ratio
				Cross sectional area (mm²)	length (mm)	P_{Exp}	P_{FEA}	P_{Exp} / P_{FEA}
1	762	46	Control	-	-	182	178	0.98
P1	762	46	Strengthened	57.5	720	191	192	1.00
P2	990	60	Strengthened	57.5	870	-		-
A3	1150	70	Control	-	-	148	145	0.98
P3	1150	70	Strengthened	57.5	1110	199	188	0.94
A5	1528	93	Control	-	-	102	100	0.98

Table 6: Summary of the FE and experimantal results

As mentioned before, the strengthened columns failed due to debonding of the CFRP layers on the compression side of the buckled column. Figure 19 compares the FE and experimental results of load-carrying capacity versus axial and lateral displacements, while Figure 18 compares the FE and Experimental results of load carrying capacity versus vertical strain of both control and strengthened specimens.
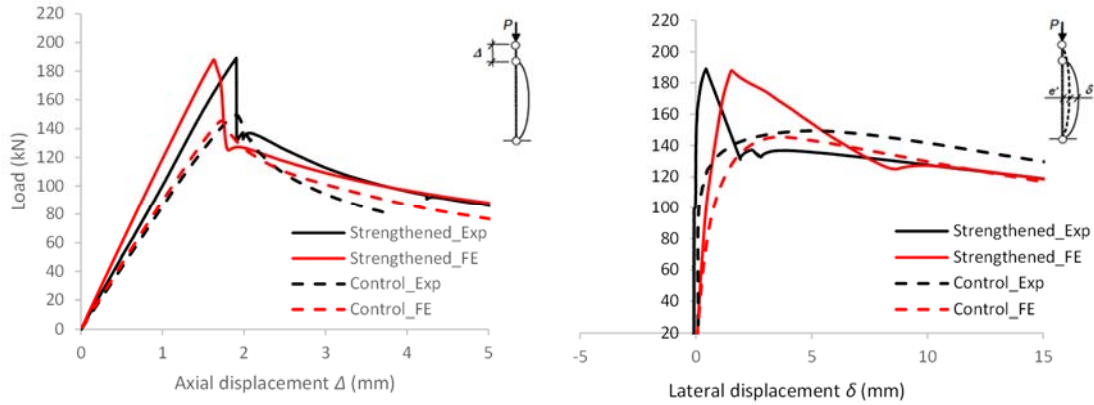
Figure 18: FE vertical strain on compression and tension sides of the specimen compared to experimental results of Shaat and Fam (2009), Slenderness ratio of 70.
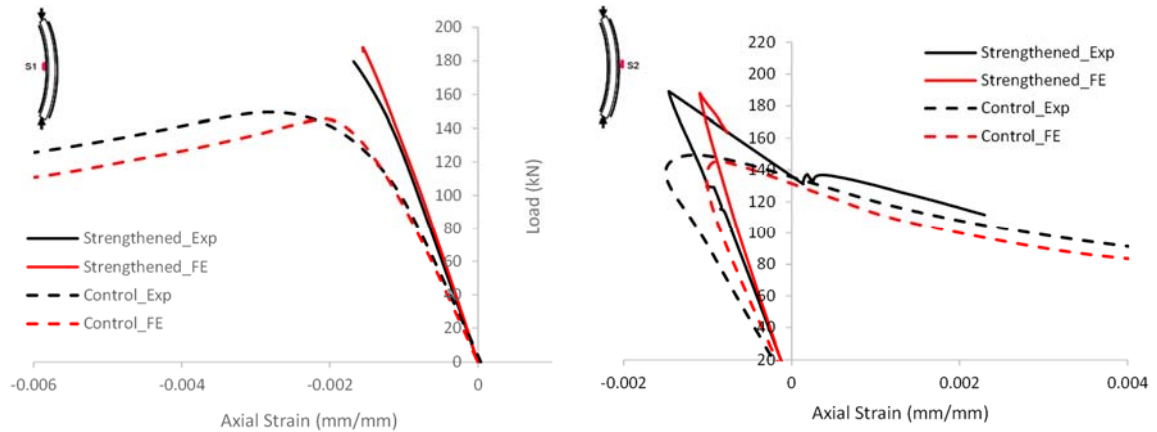
Figure 19: FE axial and lateral displacements compared to experimental results of Shaat and Fam (2009); slenderness ratio of 70

Parametric Study

A parametric study was performed on the strengthened column to evaluate the effect of CFRP length on the increase in ultimate strength. The CFRP length ranged from 20% to 100% of the complete CFRP length (L) of the specimen. Table 7 summarizes the parametric study.

Specimens	Steel column length (mm)	Slenderness ratio	CFRP area (mm²)	CFRP length (mm)	Maximum load, P_{max} (kN)	% Inc.	Axial shortening at failure (mm)
P1_0			Nil	Nil	183.29	-	1.48
P1_0.2L			57.50	144.00	181.22	0 %	1.48
P1_0.4L	762.00	46.00	57.50	288.00	178.27	0 %	1.25
P1_0.6L			57.50	432.00	189.23	3 %	1.26
P1_0.8L			57.50	576.00	192.40	5 %	1.25
P1_L			57.50	720.00	192.09	5 %	1.15
P2_0			Nil	Nil	166.50	-	1.63
P2_0.2L			57.50	180.00	160.93	0 %	1.63
P2_0.4L	990.00	60.00	57.50	360.00	169.01	2 %	1.54
P2_0.6L			57.50	540.00	177.05	6 %	1.62
P2_0.8L			57.50	720.00	185.92	12 %	1.62
P2_L			57.50	870	200.80	21 %	1.51
P3_0			Nil	Nil	145.19	-	1.71
P3_0.2L			57.50	222.00	146.74	1 %	1.61
P3_0.4L	1152.00	70.00	57.50	444.00	157.09	8 %	1.63
P3_0.6L			57.50	666.00	165.70	14 %	1.63
P3_0.8L			57.50	888.00	176.67	22 %	1.65
P3_L			57.50	1110.00	188.03	30 %	1.63

Table 7: Summary of the parametric study

Figure 20: shows the behavior of strengthened columns with different CFRP lengths for three different slenderness ratios (46, 60, and 70)
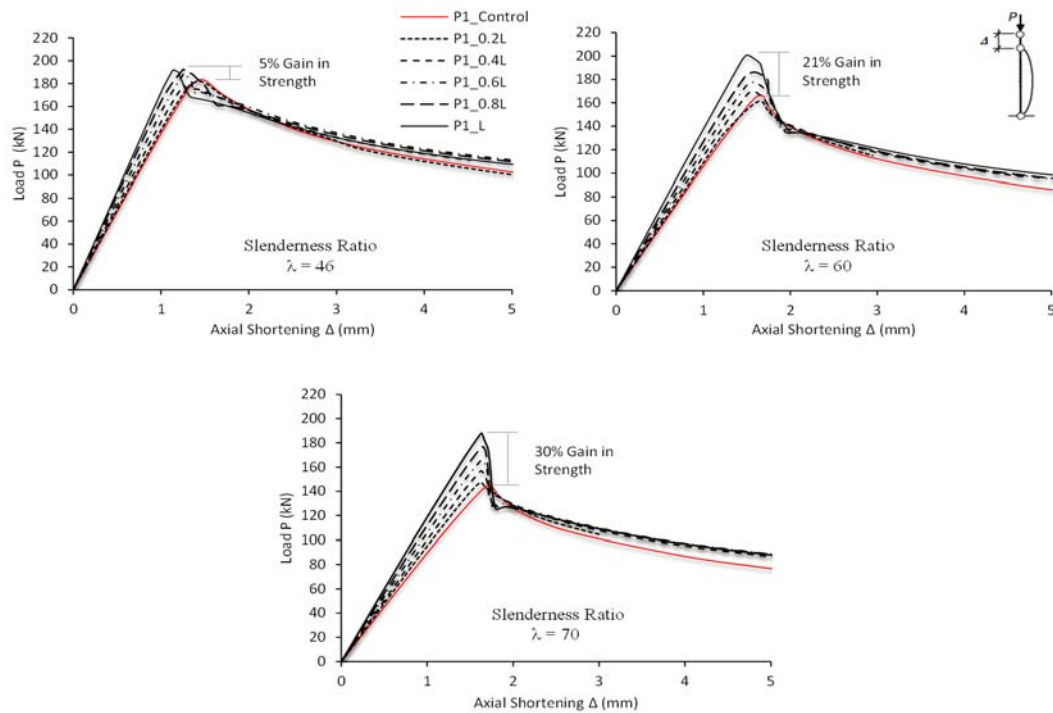

Figure 20: Behavior of strengthened columns with different CFRP lengths

Conclusion

The results of the numerical model of cold-formed HSS members strengthened using bonded CFRP reinforcement oriented in the longitudinal direction matched well with the experimental results. The following summarizes the conclusion of this work:

- Behavior of the numerical model of the control specimens, defined by using the proposed material model, initial geometric imperfections, residual stresses and associated equivalent plastic strains is in good agreement with the experimental values.
- The ultimate load capacity of the strengthened specimens defined using surface-based cohesive behaviour with mixed mode traction-separation law yielded satisfactorily close results compared to the experimental results (within 6%).
- This strengthening technique was not efficient for low slenderness ratios, i.e. 46 for all CFRP lengths used.
- CFRP length had a significant effect on the effectiveness of the strengthening technique. For a slenderness of 70 and 20% CFRP length, the results showed 1% increase in strength while for a 100% CFRP length, results showed a 30% increase in strength.
- Based on the cohesive model used, the studied columns' slenderness ratios (46 to 70) did not show a sufficient CFRP length in which increasing the CFRP length will not show increase in strengthened column strength
- Based on the cohesive model used, for all the investigated slenderness ratios, it was shown that increasing the length had a significant positive effect on the column strength up to the value of 100%

References

Barbero, E. J. (2013). Finite Element Analysis of Composite Materials Using Abaqus. CRC Press.

Cristopher, & Schafer. (2009). Direct Strength Design of Cold-Formed Steel Members with Perforations. Washington, DC: American Iron and Steel Institute.

D Fernando, T Yu, & J G. Teng. (2012). Finite element analysis of debonding failures in CFRP-strengthened rectangular steel tubes subjected to and end bearing load. 6th International Conference of FRP Composites in Civil Engineering, 1-8.

DNV-RP-C208. (n.d.). Determination of Structural Capacity by Non-Linear FE analysis Methods.

Paul E. Hess, Daniel Bruchman, Ibrahim A. Assakkaf, & Bilal M. Ayyub. (2002). Uncertainties in Material Strength, Geometric, and Load Variables. Naval Engineers Journal, 139-166.

Shaat, A. A. (2007). Structural Behaviour of Steel Columns and Steel-Concrete Composte Girders Retrofitted using FRP. Ontario, Canada: Queen's University.

Shaat, A., & Fam, A. Z. (2009). Slender Steel Columns Strengthened Using High-Modulus CFRP Plates for Buckling Control. ASCE.